Journal of Innovative Optical Health Sciences
Vol. 5, No. 4 (2012) 1250025 (9 pages)

DOI: 10.1142/S1793545812500253

DEEP-UV CONFOCAL FLUORESCENCE IMAGING AND SUPER-RESOLUTION OPTICAL MICROSCOPY OF BIOLOGICAL SAMPLES

TREVOR A. SMITH*, LIISA M. HIRVONEN, CRAIG N. LINCOLN
and XIAOTAO HAO
School of Chemistry and ARC Centre of Excellence
for Coherent X-ray Science, University of Melbourne
Parkville 3010, Australia
**trevoras@unimelb.edu.au*

Accepted 28 July 2012
Published 9 November 2012

A wide range of techniques has been developed to image biological samples at high spatial and temporal resolution. In this paper, we report recent results from deep-UV confocal fluorescence microscopy to image inherent emission from fluorophores such as tryptophan, and structured illumination microscopy (SIM) of biological materials. One motivation for developing deep-UV fluorescence imaging and SIM is to provide methods to complement our measurements in the emerging field of X-ray coherent diffractive imaging.

Keywords: Time-resolved fluorescence imaging; structured illumination microscopy.

1. Introduction

Most fields of science, including the botanical, biological, chemical and materials sciences, require information on ever-decreasing spatial scales, and a host of techniques is now at our disposal to achieve high spatial resolution, including electron, X-ray, scanning probe and various modes of optical microscopy. Optical microscopy, in particular some emission-based techniques, can provide the ability to further resolve the spatial information in the time domain, thereby providing a wealth of additional information. This is a major capability advantage over some of the other microscopy modes. However, optical microscopy methods have been restricted by the laws of diffraction in the spatial resolution they can provide to the hundreds of nanometers scale, as dictated by the Abbe diffraction limit and Rayleigh's criterion ($d \sim \frac{\lambda}{2(n \cdot \sin\theta)}$).

One approach to increasing the spatial resolution is therefore to reduce the wavelength of the radiation used, e.g., to UV or even X-ray regions. Scanning confocal fluorescence imaging is usually performed in the visible region of the spectrum, most commonly exciting exogenous fluorescent probes such as dyes, fluorescent proteins, quantum dots or nanodiamond particles. Besides any increase in spatial resolution, there are other advantages (and disadvantages) of using UV excitation, including exciting endogenous fluorophores directly into their absorption bands in the UV region. Intrinsic fluorophores, such as tryptophan, can be photoexcited directly with UV radiation and their

fluorescence imaged.[1–5] We will discuss the advantages and disadvantages of this approach and provide examples of its application in samples of biological and botanical interest. We have also extended this "deep-UV" excitation through time-resolved fluorescence measurements, with added benefits over steady-state excitation. One such advantage of time-resolving the emission is that the increased scattered light, a consequence of UV excitation compared with visible excitation, can be discriminated from emission through time gating.

A more elegant and productive approach to achieving improved spatial resolution beyond the diffraction limit is through the suite of "super-resolution" optical microscopy methods. These methods do not beat the diffraction limit; rather they utilize ingenious ways around it. The first approach to overcome the diffraction limit was scanning near-field optical microscopy (SNOM). Subsequently, techniques such as stimulated emission depletion (STED) microscopy, photoactivated localization microscopy (PALM) or stochastic reconstruction optical microscopy (STORM) and structured illumination microscopy (SIM) have gained popularity to various degrees, particularly in the biological sciences. SIM can improve the optical resolution by a factor of two and potentially more through saturated SIM. There are also potential improvements and advantages to be gained in using SIM with UV excitation. We will discuss the implementation and application of SIM for fluorescence imaging of biological samples.

2. Experimental Details

2.1. *Deep-UV confocal fluorescence imaging*

A schematic of the deep-UV time-resolved confocal fluorescence microscope is shown in Fig. 1. The instrument employed the frequency tripled output (INRAD M/N 5-050) of a mode-locked Ti:Sapphire laser (Mira 900F, Coherent) pumped by a 10 W Nd:Vanadate laser (Verdi V10, Coherent) as the illumination source (76 MHz pulse repetition rate, ~100 fs pulse duration). The frequency tripler used a 1.5-mm-thick Lithium Triborate LiB_3O_5 (LBO) crystal to generate the second harmonic light by frequency doubling and a 0.5-mm β-Barium-Borate BaB_2O_4 (BBO) crystal for sum frequency mixing to produce third harmonic light. The 280-nm light was guided to the confocal microscope optics via a cylindrical lens (to reduce astigmatism), a band-pass filter to block undesirable wavelengths reaching the microscope optics and detector, a 280-nm reflecting/>300 nm transmitting dichroic beam splitter and a spatial filter, after which it filled the back aperture of a UV microscope objective (Zeiss UltraFluar, 1.25 N.A, 100X, 160 mm tube length,

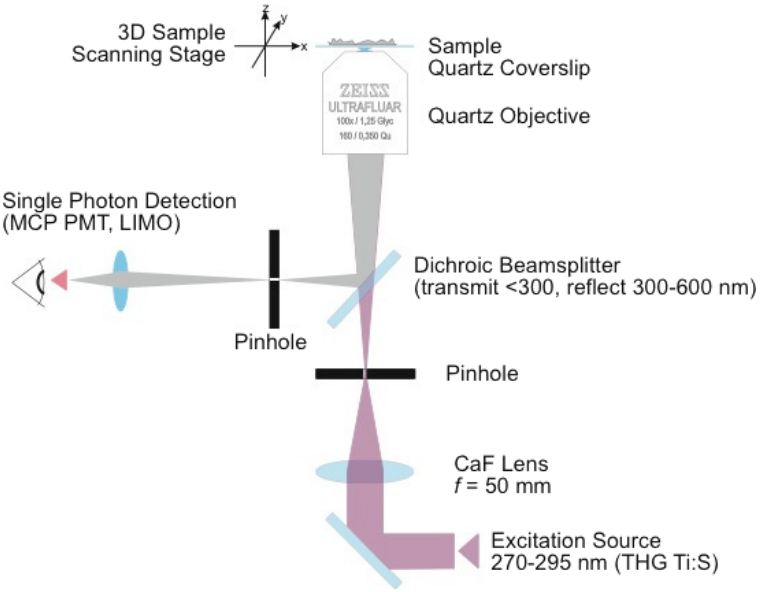

Fig. 1. Schematic of the deep-UV confocal microscope.

glycerol immersion). The excitation light was then focused onto the sample mounted on a piezo-driven X, Y, Z translation stage (Nanonics) that was in turn mounted on a tilt adjustment stage to ensure the X, Y plane was normal to the incident light. Emission was collected by the same objective, filtered through a pair of band-pass filters (WG 320 and WG 305), focused through an adjustable diameter aperture, and onto a single photon counting microchannel plate (MCP) detector (Eldy EM1-132). Fluorescence imaging was performed using a gated photon counting system (Stanford SR400) integrated with a LabView VI (National Instruments). Time-resolved imaging performed here used the four-channel gating method of Gerritsen *et al.*[6] (Fig. 2), commercialized as the Nikon LIMO system, which exploits the sensitivity of photon counting coupled with fast switching and accurate digital delay chips. This method enables the recording of time-resolved fluorescence information, on the sub-nanosecond to microsecond time-scales, on a pixel-by-pixel basis at high count rates and with high detection efficiency. The LIMO unit was synchronized to the frame, line and pixel clocks of the scan unit.

2.2. *Structured illumination microscope*

The structured illumination microscope is described in detail in Ref. 7; in brief, it uses a DPSS laser (476 nm, 300 mW, Shanghai Laser and Optics Century Co., Ltd.) delivered via an endlessly single-mode photonic crystal fiber (NKT Photonics), a fused silica transmission grating (80 lines/mm, Edmund Optics, NT57-887) mounted on a hollow axis stepper motor rotation stage (ST5918S3008-L, Nanotech) that was in turn mounted on a short motorized translation stage (Newport MFA-CC/SMC100CC). We used an objective lens (Olympus UPlanSApo 100X, 1.4 NA) with piezo-nanopositioner focusing element (MadCity Labs, NanoF Series) for excitation and emission collection. The emission was detected using an electron multiplying back illuminated CCD camera (Princeton Instruments, PhotonMax 1024B, 1024×1024, $13\,\mu$m pixels). The rotation and translation of the grating and the acquisition of the images from the EMCCD camera were controlled using software based on the MicroManager platform. Nine images (three orientations of the grating and three translations of the grating at each orientation) were collected, from which the image was reconstructed based on published procedures.[8,9]

Fig. 2. Intensity-based image of crystalline D,L-tryptophan ($10\,\mu\text{m} \times 10\,\mu\text{m}$, $\lambda_{\text{exc}} = 280\,\text{nm}$, $\lambda_{\text{em}} \sim 305{-}450\,\text{nm}$).

2.3. *Sample preparation*

The UV objective used in this work requires 350-μm-thick quartz coverslips. These were sourced from Technical Glass Products, Inc., and cleaned thoroughly prior to use with several washes in UV-grade acetone.

Several drops of dissolved D,L-Tryptophan (Sigma Aldrich, recrystallized from an aqueous solution $\geq$99%) were evaporated onto a clean coverslip. The growth of crystals was evident after this time period. A eucalyptus leaf, sectioned into $\sim$5 mm $\times$ 5 mm, was immersed in a small amount of MilliQ water and sandwiched between two coverslips. Fine chlorinated Merino wool fibers were sandwiched between two coverslips. Sterilized malarial infected red blood cell samples labeled with green fluorescent protein (GFP) were prepared by the Tilley group at La Trobe University, and simply smeared over a quartz coverslip.

3. Results and Discussion

3.1. *Deep-UV confocal fluorescence imaging*

Fluorescence imaging of biological material usually relies on the labeling of sample with exogenous fluorophores such as organic dyes, fluorescent proteins, quantum dots or, more recently, color-center-defected diamond nanoparticles. The inclusion of

the fluorophore can potentially affect what is imaged due to factors such as the size, charge or other properties of the fluorophore itself. It is therefore attractive to use the "autofluorescence" of biological samples that results from the intrinsic fluorescence of proteins, coenzymes, etc. In proteins, it is the three amino acid residues, tryptophan (Trp), tyrosine (Tyr) and phenylanaline (Phen), that contribute most to the fluorescence when excited in the 250−280 nm regime. The emission of these closely related amino acids is strongly dependent on their molecule structure. Phen has a small absorptivity (∼200 $M^{-1}\,cm^{-1}$ at 257 nm) and a low fluorescent quantum yield (∼0.04), and so is only really observed in the absence of both Tyr and Trp. Adding a hydroxyl group, as in tyrosine, causes a 20-fold increase in fluorescence signal due to the combination of increased absorptivity (∼1400 $M^{-1}\,cm^{-1}$ at 274 nm) and increased fluorescence quantum yield (∼0.14). Replacement of the phenyl ring with an indole group, as in Trp, leads to further significant increases in the relative fluorescence signal due to improved absorptivity and quantum yield (∼5600 $M^{-1}\,cm^{-1}$ at 280 nm and 0.2 nm, respectively), and so the inherent fluorescence signal is often dominated by the presence of Trp. Trp residues that are buried in the hydrophobic core of proteins can have spectra which are shifted by 10 nm to 20 nm compared to those on the surface of the protein. The intensity, quantum yield and wavelength of maximum fluorescence emission of Trp is highly solvent dependent; the fluorescence spectrum shifts to shorter wavelength and fluorescence intensity increases as solvent polarity surrounding the tryptophan residue decreases. Trp emission is also sensitive to local environment (protein folding/position), e.g., the emission of Trp is centered around 340 nm in close-packed protein and 360 nm in aqueous media.

Unfortunately, the emission from these amino acids requires photoexcitation in the UV region. One approach to overcome this is to use multi-photon imaging, which has been used to great effect, e.g., in imaging skin[10]; however, Trp has a very low two-photon absorption cross-section (∼5.81 GM),[11] rendering multi-photon imaging of Trp in biological systems exceedingly difficult, although feasible.[12] A lesser-used approach is through direct UV excitation, which we have adopted here. While it is sometimes difficult to distinguish these amino acids on the basis of their steady-state emission spectral properties, it is sometimes possible to overcome this using the difference in their fluorescence lifetime (∼6.4 ns, 3.6 ns and 2.6 ns for Phen, Tyr and Trp, respectively).[13] A fortunate consequence of using an ultrafast laser as the source of deep-UV excitation for confocal microscopy is that time-resolved fluorescence imaging can be readily invoked, providing additional information and the potential to gate out scattered light. A further possible advantage of using UV excitation is an increased resolution, which with 280 nm excitation could provide a theoretical lateral and axial resolution of ∼90 nm and 250 nm, respectively.

We have undertaken steady-state and time-resolved confocal fluorescence imaging of tryptophan-containing samples with direct excitation of the UV absorption band to assess the feasibility of this approach. An intensity-based confocal fluorescence image of crystalline D,L-tryptophan, with a pixel scan rate of 200 Hz, is shown in Fig. 2. The emission collected was from the whole band that peaks at ∼355 nm using the optical filter wavelength selection mentioned in the experimental section. This area of the sample was scanned repeatedly for over 30 min without significant photobleaching or other obvious sample damage. The crystalline structure is clearly visible, and acquisition of this test image provided the incentive that the single-photon-counting-based deep-UV confocal microscope was capable of imaging tryptophan as an inherent fluorophore, at least under these idealized conditions.

Wool fibers are composed of alpha-keratin proteins that contain many different amino acids, amongst which Trp is a major component.[14] The fibers have a complex morphological structure with the cuticle and cortical cells differing in their amino acid compositions. We have attempted to image Merino wool fibers directly using the deep-UV confocal fluorescence microscope described. Figure 3(a) shows an intensity-based scanning confocal fluorescence image of a chlorinated Merino wool fiber. The LIMO time-gated fluorescence imaging method was applied to the same fiber. In this method, four time gates (each of the channels corresponds to an increased delay of 1.2 ns following excitation), are applied and four images collected simultaneously, from which a "lifetime map" [Fig. 3(b)] can be generated. In this image the most dominant lifetime was ∼1.4 ns, and the lifetime range was from 0.5 ns to 2 ns, as determined from the fluorescence lifetime

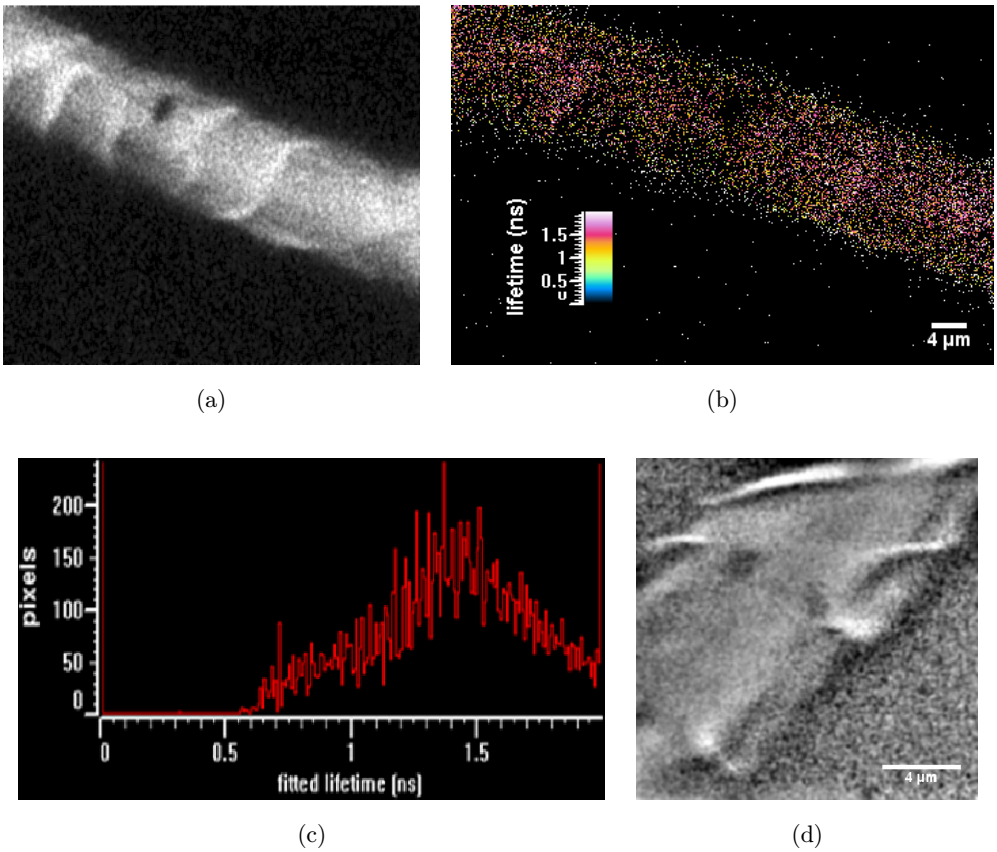

Fig. 3. (a) Intensity and (b) LIMO time-resolved fluorescence images of a Merino wool fiber ($\lambda_{exc} = 280\,nm$, λ_{em} between 300−400 nm), (c) fluorescence lifetime distribution from (c), (d) zoomed image (image size $20\,\mu m \times 20\,\mu m$ (400 pixels × 400 pixels)).

distribution calculated over the image in (b) [Fig. 3(c)]. This suggests that the most likely inherent emitter is indeed Trp. Also shown is a zoomed in image (d) of the wool fiber clearly showing the cuticle structure.

These images were taken at a pixel scan frequency of 100 Hz at 50 nm per pixel. The total image acquisition time was 60 min, and again the sample showed little sign of photodegradation over this period under the low level of UV photoexcitation and single photon detection used.

We have also applied deep-UV confocal fluorescence imaging to botanical samples. Stomata from a botanical gum leaf sample are shown in Fig. 4. This image is intensity-based, and each pixel corresponds to 100 nm scan step increments. The image acquisition time was approximately 30 min, at a scan frequency of 200 Hz, and this sample was also largely unaffected by the repeated UV scanning under these conditions. This image shows clearly the visible structures such as the pore, thickened walls on the pore, guard cells and the epidermal cells, clearly illustrating the potential of the UV confocal imaging technique to resolve the structure with botanical samples without the need for artificial fluorescence staining.

Malaria is a mosquito-borne infectious disease in which the protists first infect the liver and then act as parasites within the red blood cells. Young mosquitoes first ingest the malaria parasite by taking a blood meal from an infected vertebrate carrier. Once ingested, the parasite gametocytes taken up in the blood will further differentiate into male or female gametes and then fuse in the mosquito's gut. Plasmodium sporozoites are produced that migrate through the mosquito's body to the salivary glands. The sporozoites are injected into the skin with the saliva when the mosquito takes a subsequent blood meal. Various modes of microscopy have been exploited to image various aspects of the life cycle of the malaria parasite, and to this we add deep-UV fluorescence imaging of a malarial-infected red blood cell (Fig. 5). In this case the red blood cell was artificially stained with GFP

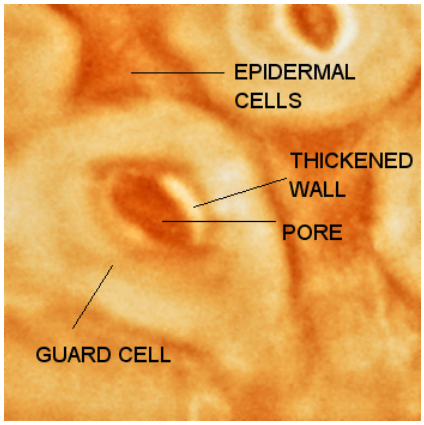

Fig. 4. Stomata in a gum leaf sample.

but excited at 280 nm rather than in the conventionally used visible region. The dark regions in the cell indicate sites of infection of the protozoan parasite. Two prominent lifetimes are evident in the lifetime distribution in the time-resolved fluorescence image. At sites of parasitic infection and around the red blood cells edges a lifetime of ∼0.85 ns is dominant, whereas a decay component of ∼0.6 ns is visible throughout the red blood cell. This larger lifetime around sites of parasitic infection is an indication that the chemical environment surrounding the parasite is altered compared to the unaffected cells.

3.2. *Structured illumination microscopy*

Super-solution optical microscopy methods are providing a level of detail only dreamed about only a few years ago. Each method has its advantages and disadvantages, particularly for a given type of sample, and in terms of the information required. Of the range of super-resolution optical microscopy methods, despite its less celebrated (compared to STED or PALM) improvements in spatial resolution over conventional imaging (being limited to a factor of approximately two in each dimension), SIM affords several advantages that make it the method of choice in many circumstances. Key factors include its wide-field nature, which therefore makes it comparatively rapid and less phototoxic,

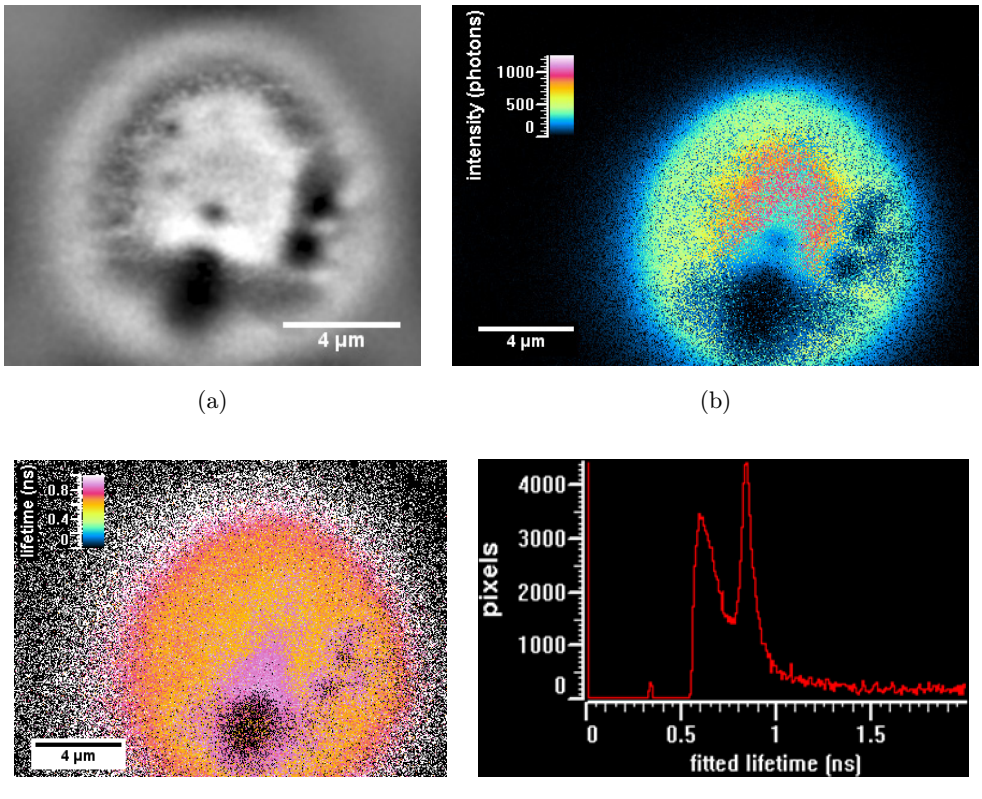

(a) (b)

(c) (d)

Fig. 5. Malarial infected red blood cell: (a) intensity-based image, (b) integrated time-resolved image, (c) LIMO-generated fluorescence lifetime map, (d) fluorescence lifetime distribution from (c).

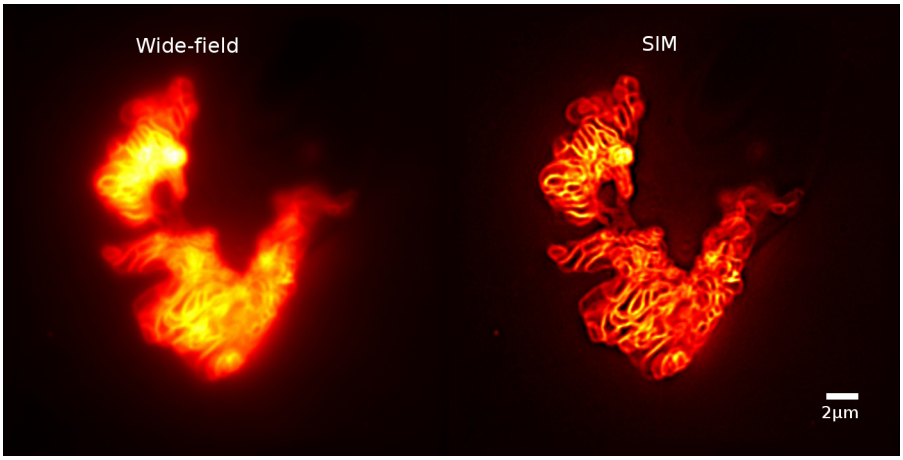

Fig. 6. Wide-field and SIM fluorescence images of GFP-labeled mitochondria in COS7 cells. ($\ddot{e}_{exc} = 476$ nm, sample L. Osellame and M. Ryan, La Trobe University).

and the fact that it can be used with any fluorophore. We have applied SIM to a wide range of samples, from conjugated polymers to botanical and biological samples. We present here a couple of examples that illustrate the improvement in spatial resolution achievable with SIM over conventional, wide-field microscopy.

Mitochondria are sometimes described as "cellular power plants" because they generate most of the cell's supply of ATP, used as a source of chemical energy. In addition to supplying cellular energy, mitochondria are involved in a range of other processes, such as signaling, cellular differentiation, cell death as well as the control of the cell cycle and cell growth. Figure 6 compares the conventional wide-field and SIM fluorescence images of GFP-labeled mitochondria in COS7 cells. The improvement in resolution is clear.

As discussed earlier, the life cycle of the malarial-infected red blood cell involves the production of gametocytes. Figure 7 compares the conventional wide-field and SIM fluorescence images of gametocytes in fixed malaria-infected red blood cells labeled with GFP, again excited with 476 nm radiation.

It is worth noting that the GFP emission of extrinsically labeled samples such as that of the previous two examples, could potentially also be induced with UV excitation, but this was not used in this instance. We have attempted to implement SIM with deep-UV excitation using the frequency tripled output of the mode-locked titanium sapphire laser and the UV-enhanced Photon Max EMCCD camera (Fig. 8), but with only limited success to date. This approach does offer the possibility of increased spatial resolution through the UV

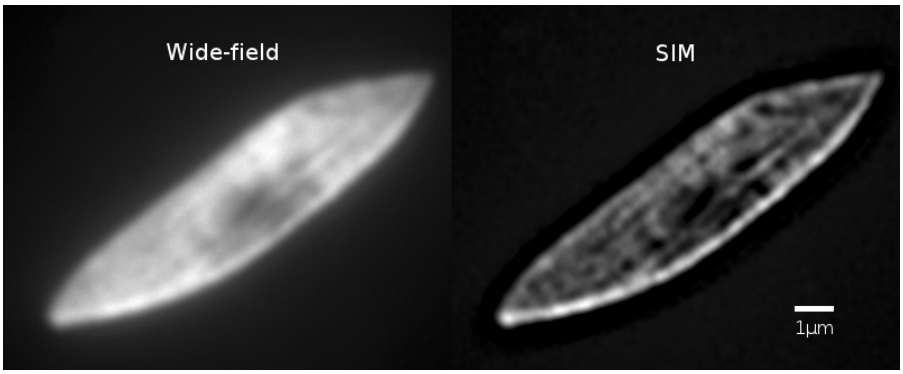

Fig. 7. Wide-field and SIM fluorescence images of gametocytes in fixed malaria-infected red blood cells labeled with GFP. (Sample: M. Dearnley and L. Tilley, La Trobe University).

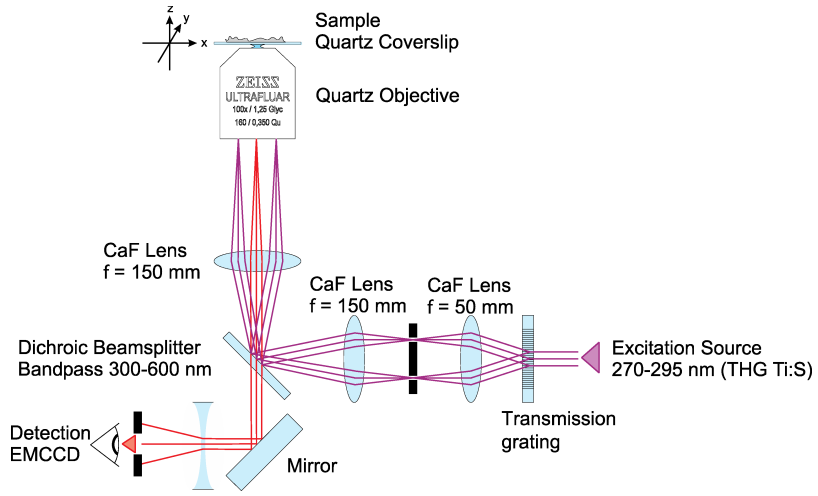

Fig. 8. Deep-UV structured illumination microscope.

wavelengths used and the advantages of SIM. A further advantage related to the wide-field nature of SIM as compared with single point scanning of confocal microscopy, potentially leading to less sample damage. This technique may also have applications in studying polymer thin films.

4. Conclusions

This investigation has shown that deep-UV confocal microscopy using a mode-locked laser is a potentially powerful yet largely unexplored technique that can be used to image samples containing inherent fluorophores under certain circumstances. Time-resolved fluorescence imaging, which is a natural extension of using mode-locked pulses as the excitation source, enables one to gain an understanding of the various chemical environments and how processes may cause disruption to these regions. It has been shown that time-resolved deep-UV confocal fluorescence imaging can be successfully applied to a wide range of samples and is promising for some (although probably limited) biological samples. Implementation of this imaging technique into the biological sciences could be advantageous due to the additional information obtainable and the lack of need to label samples with fluorophores, which can cause undesirable processes due to the label affecting the chemistry of the sample. The method's real benefit probably lies in the botanical and advanced materials sciences.

Super-resolution optical microscopy methods are already making significant contributions to imaging biological samples and can potentially play a role in the botanical and materials sciences. Of the methods available, SIM exhibits some advantages for the types of samples currently under investigation and still has some further developments that could add to its attractiveness.

The real potential of these techniques may well be more fully realized when used in a "correlative" mode, i.e., in conjunction with other imaging modes such as coherent diffractive imaging or electron microscopy, to provide complementary information.

Acknowledgments

We acknowledge the support of the Australian Research Council for the Center of Excellence for Coherent X-ray Science (CE0561787). We also acknowledge collaborations with the groups of Prof. M. Ryan (La Trobe University), Prof. L. Tilley (La Trobe University/University of Melbourne). We also acknowledge Peter Wichta and Niels Zijlstra for assistance in some of the deep-UV imaging.

References

1. Q. Li, T. Ruckstuhl, S. Seeger, "Deep-UV laser-based fluorescence lifetime imaging microscopy of single molecules," *J. Phys. Chem. B* **108**, 8324−8329 (2004).
2. Q. Li, S. Seeger, "Label-free detection of single protein molecules using deep UV fluorescence lifetime microscopy," *Anal. Chem.* **78**, 2732−2737 (2006).

3. M. Schüttpelz, C. Müller, H. Neuweiler, M. Sauer, "UV fluorescence lifetime imaging microscopy: A label-free method for detection and quantification of protein interactions," *Anal. Chem.* **78**, 663−669 (2006).
4. T. A. Smith, C. N. Lincoln, D. K. Bird, Time-Resolved Fluorescence in Microscopy, in *Fluorescence Applications in Biotechnology and Life Sciences*, E. M. Goldys, Ed., Chap. 10, pp. 195−221, Wiley-Blackwell (2009).
5. C. J. R. van der Oord, *Confocal Imaging and Microvolume Spectroscopy Using Synchrotron Radiation*, Cip-Data Koninklijke Bibliotheek, Den Haag (1994).
6. C. J. de Grauw, H. C. Gerritsen, "Multiple time-gate module for fluorescence lifetime imaging," *Appl. Spectr.* **55**, 670−678 (2001).
7. X. T. Hao, L. M. Hirvonen, T. A. Smith, Nanomorphology of polythiophene-fullerene bulk-heterojunction films investigated by structured illumination optical imaging and time-resolved confocal microscopy, (submitted).
8. M. G. L. Gustafson, D. A. Agard, J. W. Sedat, Three-dimensional and multidimensional microscopy: Image acquisition processing VI, Vol. 3919, in *Proc. SPIE*, J.-A. Conchelo, C. J. Cogswel, T. Wilson, Eds., pp. 141−150 (2000).
9. R. Heintzmann, T. M. Jovin, C. Cremer, "Saturated patterned excitation microscopy — a concept for optical resolution improvement," *J. Opt. Soc. Am. A* **19**, 1599−1609 (2002).
10. D. K. Bird, A. L. Schneider, A. Watkinson, B. Finnin, T. A. Smith, "Navigating transdermal diffusion with multiphoton fluorescence lifetime imaging," *J. Microscopy.* **230**, 61−69 (2008).
11. T. A. Smith, C. N. Lincoln, *Determination of 2-Photon Absorption Cross-Section of Tryptophan*, unpublished.
12. M. Lippitz, W. Erker, H. Decker, K. E. van Holde, T. Basche, "Two-photon excitation microscopy of tryptophan-containing proteins," *Proc. Natl. Acad. Sci.* **99**, 2772−2777 (2002).
13. G. Mocz, Intrinsic fluorescence of proteins and peptides, available at http://dwb.unl.edu/Teacher/NSF/C08/C08Links/pps99.cryst.bbk.ac.uk/projects/gmocz/fluor.htm. (2012).
14. D. R. Graham, K. W. Statham, "Trptophan in wool. Part 1: Determination of the tryptophan contect of wool," *Text. Res. J.* **30**, 136−139 (1960).